Table 3 Univariate analysis for overall survival of patients with DLBCL-EH and DLBCL-CG

Characteristic	No. of patients	Five-year OS (%)	*P* value
Age, years			
Age≦60	43	60.2	NS
Age > 60	75	51.1	
Sex			
Male	66	52.4	NS
Female	52	57.8	
Primary site			
Nodal	55	55.2	NS
Extranodal	38	67.7	
Serum LDH level			
Normal or lower	59	72.4	0.0014
Higher than normal	59	38.3	
Performance status			
ambulatory (0–1)	88	67.0	<0.001
not ambulatory (2–4)	30	13.7	
Ann Arbor stage			
Stage 1/2	61	72.8	<0.001
Stage 3/4	57	34.1	
Extranodal involvement			
0–1 site	90	63.6	<0.001
> 1 sites	28	25.0	
International Prognostic Index			
L/LI	70	75.9	<0.001
HI/H	48	23.2	
GCB/non-GCB			
GCB	52	65.7	0.017
Non-GCB	61	45.6	
Prominent epithelioid cell response			
Present	22	85.9	0.045
Absent	96	50.0	

DLBCL-EH diffuse large B-cell lymphoma (DLBCL) with a high number of epithelioid histiocytes; *DLBCL-CG* DLBCL-control group, *OS* overall survival, *L/LI* low/low-intermediate, *HI/H*, high-intermediate/high, *GCB* germinal center B-cell type, *NS* not significant

cells as shown in Fig. 1a and e. Marked appearance of cluster of epithelioid histiocytes, as shown in this study (Fig. 1), is not described and illustrated. Lymphoepithelioid B-cell lymphoma was differentiated from THRLBCL by predominance of histiocytes to small lymphocytes and their epithelioid morphologies, not by percentages of histiocytes and lymphocytes in the present study as also in the study by Achten et al. [11]. Achten et al. described that histiocytes in their cases with histiocyte-rich, T-cell-rich B-cell lymphoma, which corresponds to the THRLBCL, were not epithelioid in appearances. Chetaille et al. [12] reported that the T cells in all of THRLBCL cases expressed PD-1 antigen. This showed a clear contrast to the present cases, in which only three of 21 cases were PD-1 positive.

Table 4 Multivariate analysis of clinicopathological factors for overall survival of patients with DLBCL-EH and DLBCL–CG

Characteristic	Relative risk	95% CI	*P* value
Serum LDH level>normal	1.43	0.65–3.15	NS
Performance status 2–4	2.95	1.52–5.72	0.0014
Stage 3/4	1.88	0.61–5.85	NS
Involved extranodal organ>1	1.77	0.88–3.56	NS
IPI, HI/H	1.34	0.34–5.32	NS
Germinal center B-cell type	0.53	0.28–1.03	0.062
Prominent epithelioid cell response	0.26	0.077–0.86	0.028

DLBCL-EH diffuse large B-cell lymphoma (DLBCL) with a high number of epithelioid histiocytes, *DLBCL-CG* DLBCL control group, *CI* confidence interval, *IPI* International prognostic index, *HI/H* high-intermediate/high, *NS* not significant

Some of the similar cases to the present series were included in the previous reports under the headings of TCR-, T/HR- or TC/HR-(L)BCL [13–15], but prognosis of this special type of THRLBCL was not commented in comparison with representative cases of THRLBCL without prominent epithelioid reaction. Large B-cell lymphomas generally fail to provoke a substantial immune reaction; therefore, prominent epithelioid cell reaction is exceptional: Frequency of DLBCL-EH among all DLBCL cases registered with the OLSG is only 1.8%.

Patients with DLBCL-EH showed the significantly favorable prognosis than those with DLBCL-CG, i.e., ordinary type of DLBCL. This finding contrasts to the disease diagnosed as THRLBCL by the WHO criteria, which shows similar prognosis to stage- and IPI-matched ordinary DLBCL [15–18]. The present multivariate analysis revealed that the prominent epithelioid cell response was an independent factor for favorable prognosis. The present clonality analysis based on the Ig gene rearrangement confirmed the clonal nature of B-cell proliferation in the DLBCL-EH. Proliferative activity, as revealed by MIB-1 labeling index, was rather similar between DLBCL-EH and DLBCL-CG. It has been reported that DLBCL of non-GCB subgroup showed a more unfavorable prognosis than that of GCB subgroup [4, 9, 19]. Frequency of GCB and non-GCB cases in the present series was rather similar, which is identical to the previous reports on DLBCL [3].

DLBCL is divided into the two types based on the gene expression profiles of the proliferating cells, i.e., GCB type and ABC with more favorable prognosis of the former than the latter type [3, 4]. Recently, Lenz et al. [20] reported that DLBCL could be categorized based on the gene expression signatures of stromal cells surrounding the neoplastic large B-lymphoid cells. The stromal cell gene signature found in cases showing histiocyte-rich host reaction to the lymphoma cells was correlated with favorable prognosis of the patients. This finding is concordant with the present finding that DLBCL-EH shows a favorable prognosis.

DLBCL-EH is characterized by a predominantly nodal presentation and higher EBV positive rate compared to DLBCL-CG. EBV positive rate in the ordinary type of DLBCL is reported to be less than 10% worldwide. Therefore, the higher EBV-positive rate in the DLBCL-EH is unique. One of the present patients with EBV-positive DLBCL-EH showed the spontaneous regression without adjuvant therapy. Spontaneous regressions of EBV-positive DLBCL were reported previously [21, 22], but their histologies were not epithelioid rich.

Present findings suggest that DLBCL-EH could be a morphological variant of DLBCL that has an apparent better clinical outcome than conventional DLBCL. The peculiar morphological aspect of the tumor raises several important differential diagnoses. Then, differential points of this lymphoma from other types of diseases are discussed below. Firstly, distinction of DLBCL-EH from the lymphoepithelioid cell variant of peripheral T-cell lymphoma, not otherwise specified (PTCL-NOS) is necessary. Indeed, the authors, as the pathology board members of the OLSG, initially interpreted the histologic pictures of DLBCL-EH as the lymphoepithelioid cell variant of PTCL-NOS on the purely morphological grounds. However, the immunohistochemistry revealed the B-cell nature of the proliferating large lymphoid cells. In addition, genotypic study confirmed the clonal proliferation of B cells. The presence of fine fibrous tissues and necrotic foci might be frequent to occasional in DLBCL-EH but uncommon in the lymphoepithelioid cell variant of PTCL-NOS.

Classical HL of mixed cellularity type (CHL-MC) occasionally show the histology containing a high content of epithelioid histiocytes, with rather favorable clinical course than ordinary CHL-MC [23]. Thus, distinction of DLBCL-EH from CHL-MC may be needed in some cases. Indeed, Reed–Sternberg cell-like cells appeared in the recurrent lesion of one of the present cases. However, diagnostic Reed–Sternberg cells were absent even in this lesion. Such kind of cells was never found in the initial biopsy of any cases. Complete absence of CD15-positive cells and presence of CD30-positive cells in a quite limited number of the present DLBCL-EH cases indicated that a diagnosis of CHL-MC was unlikely. CD30 immunoreactivity seems not to be a distinguishing feature of CHL, as it may be observed in the THRLBCL as well [11]. In addition, clonal B-cell proliferation was confirmed in all of the DLBCL-EH cases examined. Although mononuclear Hodgkin and multinucleated Reed–Sternberg (HRS) cells contain monoclonal Ig gene in greater than 98% of cases and monoclonal T-cell receptor gene in rare cases in the DNA isolated from the single HRS cells, the monoclonal rearrangements are usually not detectable in the whole tissue DNA [24]. With combination of histologic, immunohistologic findings and genotypic study, distinction of DLBCL-EH from CHL-MC with a high content of epithelioid histiocytes is possible.

In conclusion, the DLBCL-EH is distinct from ordinary DLBCL in its higher EBV-positive rate, predominant nodal presentation, and favorable prognosis. Because the follow-up period in the present series was rather short, further study on the DLBCL-EH with more high number of cases and adequately long follow-up period would provide a robust conclusion.

Acknowledgements The authors thank Ms. T. Sawamura, M. Sugano, K. Fujikawa, and E. Maeno for their technical assistance and Mr. Toshimitsu Hamasaki, Department of Biomedical Statistics, Osaka University, for advice on the statistical analyses. This study is supported in part by a Grant from the Ministry of Education, Culture, Sports, and Science (20014012), Japan

Conflict of interest statement We declare that we have no conflict of interest.

References

1. Stein H, Warnke RA, Chan WC et al (2008) Diffuse large B-cell lymphoma, not otherwise specified. In: Swerdlow SH et al (eds) WHO classification of tumours of haematopoietic and lymphoid tissues. World health organization classification of tumours, 4th edn. IARC, Lyon, pp 233–237
2. The Non-Hodgkin's Lymphoma Classification Project (1997) A clinical evaluation of the International Lymphoma Study Group classification of non-Hodgkin's lymphoma. Blood 89:3909–3918
3. Rosenwald A, Wright G, Chan WC et al (2002) The use of molecular profiling to predict survival after chemotherapy for diffuse large-B-cell lymphoma. N Engl J Med 346:1937–1947
4. Alizadeh AA, Eisen MB, Davis RE et al (2000) Distinct types of diffuse large B-cell lymphoma identified by gene expression profiling. Nature 403:503–511
5. The International Non-Hodgkin's Lymphoma Prognostic Factors Project (1993) A predictive model for aggressive non-Hodgkin's lymphoma. N Engl J Med 329:987–994
6. Cheson BD, Horning SJ, Coiffier B et al (1999) Report of an international workshop to standardize response criteria for non-Hodgkin's lymphomas. NCI Sponsored International Working Group. J Clin Oncol 17:1244–1253
7 Weiss LM, Jaffe ES, Liu XF, Chen YY, Shibata D, Medeiros LJ (1992) Detection and localization of Epstein–Barr viral genomes in angioimmunoblastic lymphadenopathy and angioimmunoblastic lymphadenopathy-like lymphoma. Blood 79:1789–1795
8. Van Dongen JJ, Langerak AW, Brüggemann M et al (2003) Design and standardization of PCR primers and protocols for detection of clonal immunoglobulin and T-cell receptor gene recombinations in suspect lymphoproliferations: report of the BIOMED-2 Concerted Action BMH4-CT98–3936. Leukemia 17:2257–2317
9. Hans CP, Weisenburger DD, Greiner TC et al (2004) Confirmation of the molecular classification of diffuse large B-cell lymphoma by immunohistochemistry using a tissue microarray. Blood 103:275–282
10. De Wolf-Peeters C, Delabie J, Campo E et al (2008) T cell/histiocyte-rich large B-cell lymphoma. In: Swerdlow SH et al (eds) WHO classification of tumours of haematopoietic and lymphoid tissues. World health organization classification of tumours, 4th edn. IARC, Lyon, pp 238–239
11. Achten R, Verhoef G, Vanuytsel L, De Wolf-Peeters C (2002) Histiocyte-rich, T-cell-rich B-cell lymphoma: a distinct diffuse large B-cell lymphoma subtype showing characteristic morphologic and immunophenotypic features. Histopathology 40:31–45
12. Chetaille B, Bertucci F, Finetti P et al (2009) Molecular profiling of classical Hodgkin lymphoma tissues uncovers variations in the tumor microenvironment and correlations with EBV infection and outcome. Blood 113:2765–2775
13. Macon WR, Williams ME, Greer JP, Stein RS, Collins RD, Cousar JB (1992) T-cell-rich B-cell lymphomas. A clinicopathologic study of 19 cases. Am J Surg Pathol 16:351–363
14. Baddoura FK, Chan WC, Masih AS, Mitchell D, Sun NC, Weisenburger DD (1995) T-cell-rich B-cell lymphoma. A clinicopathologic study of eight cases. Am J Clin Pathol 103:65–75
15. Abramson JS (2006) T-cell/histiocyte-rich B-cell lymphoma: biology, diagnosis, and management. Oncologist 11:384–392
16. Bouabdallah R, Mounier N, Guettier C et al (2003) T-cell/histiocyte-rich large B-cell lymphomas and classical diffuse large B-cell lymphomas have similar outcome after chemotherapy: a matched-control analysis. J Clin Oncol 21:1271–1277
17 Akı H, Tuzuner N, Ongoren S et al (2004) T-cell-rich B-cell lymphoma: a clinicopathologic study of 21 cases and comparison with 43 cases of diffuse large B-cell lymphoma. Leuk Res 28:229–236
18. El Weshi A, Akhtar S, Mourad WA et al (2007) T-cell/histiocyte-rich B-cell lymphoma: clinical presentation, management and prognostic factors: report on 61 patients and review of literature. Leuk Lymphoma 48:1764–1773
19. Sjö LD, Poulsen CB, Hansen M, Møller MB, Ralfkiaer E (2007) Profiling of diffuse large B-cell lymphoma by immunohistochemistry: identification of prognostic subgroups. Eur J Haematol 79:501–507
20. Lenz G, Wright G, Dave SS et al., Lymphoma/Leukemia Molecular Profiling Project (2008) Stromal gene signatures in large-B-cell lymphomas. N Engl J Med 359:2313–2323
21. Abe R, Ogawa K, Maruyama Y, Nakamura N, Abe M (2007) Spontaneous regression of diffuse large B-cell lymphoma harbouring Epstein–Barr virus: a case report and review of the literature. J Clin Exp Hematopathol 47:23–26
22. McCabe MG, Hook CE, Burke GA (2008) Spontaneous regression of an EBV-associated monoclonal large B cell proliferation in the mastoid of a young child following surgical biopsy. Pediatr Blood Cancer 51:557–559
23. Sacks EL, Donaldson SS, Gordon J, Dorfman RF (1978) Epithelioid granulomas associated with Hodgkin's disease: clinical correlations in 55 previously untreated patients. Cancer 41. 562–567
24. Stein H, Delsol G, Pileri SA et al (2008) Classical Hodgkin lymphoma, introduction. In: Swerdlow SH et al (eds) WHO classification of tumours of haematopoietic and lymphoid tissues. World health organization classification of tumours, 4th edn. IARC, Lyon, pp 326–329

ANTIMICROBIAL AGENTS AND CHEMOTHERAPY, Oct. 2009, p. 4559–4562 Vol. 53, No. 10
0066-4804/09/$08.00+0 doi:10.1128/AAC.01404-08

Antifungal Activity of Micafungin in Serum▽

Jun Ishikawa,[1] Tetsuo Maeda,[1] Itaru Matsumura,[1]* Masato Yasumi,[1] Hidetoshi Ujiie,[1] Hiroaki Masaie,[1] Tsuyoshi Nakazawa,[1] Nobuo Mochizuki,[2] Satoshi Kishino,[2] and Yuzuru Kanakura[1]

Department of Hematology and Oncology, Osaka University School of Medicine, Osaka, Japan,[1] and Department of Medication Use Analysis and Clinical Research, Meiji Pharmaceutical University, Tokyo, Japan[2]

Received 20 October 2008/Returned for modification 18 January 2009/Accepted 5 August 2009

We have evaluated the antifungal activity of micafungin in serum by using the disk diffusion method with serum-free and serum-added micafungin standard curves. Serum samples from micafungin-treated patients have been shown to exhibit adequate antifungal activity, which was in proportion to both the applied dose and the actual concentration of micafungin measured by high-performance liquid chromatography. The antifungal activity of micafungin in serum was also confirmed with the broth microdilution method.

Micafungin has been shown to bind to serum proteins at a level of 99.8% (13). If the unbound drug contributes to its pharmacological activity (the free-drug hypothesis), only 0.2% of total micafungin would be available to exert antifungal activity in the presence of serum, and the MIC for micafungin in vitro would increase 500-fold. However, several studies have shown that this ratio varies from 4- to 267-fold (6, 7, 11), indicating that the antifungal activities of micafungin in serum may not follow the free-drug hypothesis; instead, observed activities are mostly superior to those predicted. Furthermore, it remains unclear whether these results can be applied to micafungin in a patient's serum. To address this issue, we collected serum samples from micafungin-treated patients and examined the relationship between micafungin concentration and its in vitro antifungal activity in serum.

This study was approved by the institutional review board, and informed consent was obtained from each patient. Patients with hematologic malignancies, admitted into Osaka University Medical Hospital, were administered micafungin at a dose of 50 to 300 mg/body once daily. The efficacy of prophylaxis was defined as the absence of proven, probable (EORTC-IFICG/NIAID-MSG) (1), or suspected (unexplained persistent fever and clinical findings) (10) fungal infection, through

TABLE 1. Patient background

Patient no.	Age (yr)	Gender[a]	BW[b] (kg)	Diagnosis[c]	HSCT[d]	Antifungal treatment	Dose of micafungin (mg/body)	Duration of therapy (days)	Clinical efficacy
1	43	M	76	ML	Auto-PBSCT	Preemptive therapy	300	11	Effective
2	59	F	52	ML	Auto-PBSCT	Preemptive therapy	300	8	Effective
3	33	M	52	MS	Allo-BMT	Empirical therapy	75	55	Effective
4	51	F	47	ML	Allo-BMT	Empirical therapy	50	9	
							150	16	Effective
							225	20	
							150	4	
5	47	F	58	ML	Auto-PBSCT	Empirical therapy	150	21	Effective
							300	7	
6	22	F	45	AML	Allo-BMT	Prophylaxis	50	22	Effective
							100	6	
7	46	F	43	ALL	Allo-BMT	Prophylaxis	50	22	Effective
							100	9	

[a] M, male; F, female.
[b] BW, body weight.
[c] ML, malignant lymphoma; MS, myelodysplastic syndrome; AML, acute myeloid leukemia; ALL, acute lymphoblastic leukemia.
[d] HSCT, hematopoietic stem cell transplantation; PBSCT, peripheral blood stem cell transplantation; BMT, bone marrow transplantation.

* Corresponding author. Mailing address: Department of Hematology and Oncology, Osaka University School of Medicine, 2-2, Yamada-oka, Suita, Osaka 565-0871, Japan. Phone: 81-6-6879-3871. Fax: 81-6-6879-3879. E-mail: matumura@bldon.med.osaka-u.ac.jp.
▽ Published ahead of print on 17 August 2009.

TABLE 2. Antifungal activities and inhibitory titers of serum samples from patients administered micafungin

Patient no.	Dose of micafungin		Collection point		Antifungal activity of serum samples (μg/ml) measured using:			Ratio (%) of antifungal activities measured by:		Serum inhibitory titer
						Disk diffusion method[c]				
	mg	mg/kg	Day	Time	HPLC	Serum-free standard curve	Serum-added standard curve	Serum-free standard curve/HPLC[a]	Serum-added standard curve/HPLC[b]	
1	300	3.9	10	Peak	34.2	ND	ND			32
2	300	5.8	8	Peak	33.6	ND	ND			32
3	75	1.4	45	Peak	6.7	2.5	4.2	38	63	4
4	225	4.8	43	Peak	37.1	14.1	34.8	38	94	32
5	150	2.6	12	Peak	16.4	6.0	22.1	37	135	16
6	50	1.1	8	Trough	2.7	1.1	2.1	42	78	2
			8	Peak	8.4	3.8	8.1	42	96	8
			15	Trough	3.0	1.0	1.7	32	58	4
			15	Peak	5.6	2.5	5.2	45	92	8
7	50	1.2	15	Trough	2.3	0.9	1.6	40	71	2
			15	Peak	6.4	3.3	7.0	52	109	4
			17	Trough	2.0	ND	ND			2
			17	Peak	6.5	2.9	5.9	44	91	8

[a] Mean ± standard deviation is 41% ± 6%.
[b] Mean ± standard deviation is 89% ± 23%.
[c] These serum concentrations were estimated using the two standard curves. ND, not determined.

the end of therapy. The efficacy of the drug for suspected fungal infections was indicated by improvement of persistent fever and clinical findings.

Blood samples were collected from patients just before (trough) and after (peak) micafungin infusion, at least 4 days after initiating treatment (steady state) (2). Micafungin concentration in serum was measured by high-performance liquid chromatography (HPLC) (9, 12). The disk diffusion method was performed according to National Committee for Clinical Laboratory Standards (NCCLS) M44-A guidelines (5). To obtain standard curves, we prepared two types of serial dilution disks impregnated with micafungin standard solution, one in RPMI 1640 (serum-free standard) and the other in heat-inactivated serum from volunteers (serum-added standard). Disks were applied to Sabouraud dextrose agar plates inoculated with *Candida albicans* FP633, a clinical isolate kindly provided by Astellas Pharma Inc., Tokyo, Japan. The diameter of the area of complete growth inhibition (inhibitory zone) was measured. Similarly, disks were impregnated with serum samples collected from patients, and the inhibitory zones were measured. The determination of antifungal activity of micafungin in a patient's serum was based on two standard curves, as described above. To determine the inhibitory titer in a patient's serum, we utilized the broth microdilution method based on the guidelines in NCCLS M27-A2 (4). Serum from a patient was serially diluted twofold with serum from a volunteer, supplemented with 20 mM HEPES, and inoculated with *C. albicans* FP633. MIC was defined as the lowest concentration where no visible growth was observed. Serum inhibitory titers were defined as the highest dilution of serum that completely inhibited fungal growth.

In all seven patients, micafungin was effective for prophylaxis or treatment against fungal infections (Table 1). Serum peak concentrations (C_{max}) of micafungin (measured by HPLC) ranged from 5.59 to 37.1 μg/ml at a dose of 50 to 300 mg/body and closely correlated with both daily dose and dosage in terms of body weight (Table 2). Standard curves were prepared from both serum-free and serum-added micafungin standard disks (Fig. 1). The antifungal activity of micafungin remained intact in serum: 20 to 50% (by measured value) or 25 to 30% (by standard curve).

Results for all seven successfully treated patients are summarized in Table 2, as are the micafungin concentrations in serum samples measured by HPLC. The antifungal activity of micafungin in serum samples from these patients was 41% ± 6% (mean value ± standard deviation, ranging from 37% to 52%) of the actual micafungin serum concentration (the ratio

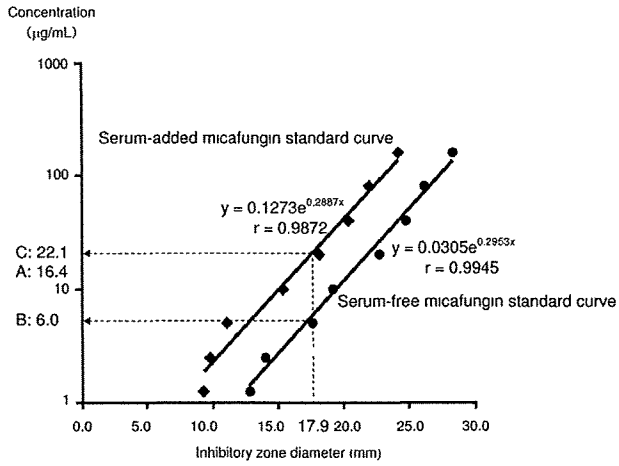

FIG. 1. Estimation of micafungin concentration in serum samples from patient no. 5, using the disk diffusion method. (A) Concentration measured using HPLC, 16.4 μg/ml. (B) Concentration estimated from the serum-free micafungin standard curve, 6.0 μg/ml. (C) Concentration estimated from the serum-added micafungin standard curve, 22.1 μg/ml. Ratio of concentration B to concentration A (%) = 6.0/16.4 × 100 = 37. Ratio of concentration C to concentration A (%) = 22.1/16.4 = 134.8.

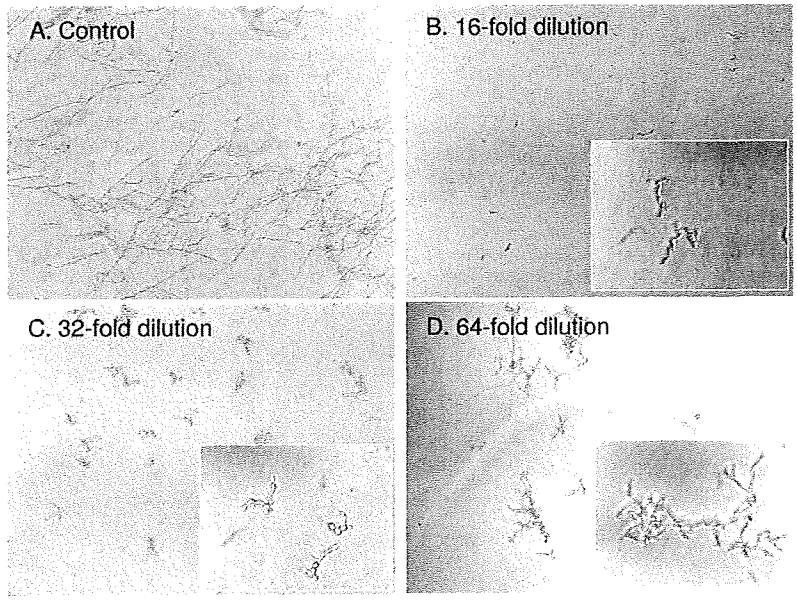

FIG. 2. Determining the inhibitory titer values for serum from patient no. 5 using the broth microdilution method. MIC was defined as the lowest concentration at which no visible growth was observed (magnification of ×40). Serum inhibitory titers were defined as the highest dilution of serum that completely inhibited fungal growth. Insets show *C. albicans* morphologies (magnification of ×400).

of antifungal activity estimated by the disk diffusion method based on the serum-free standard curve to that measured by HPLC). Representative results for patient no. 5 are shown in Fig. 1. Meanwhile, the antifungal activity of micafungin calculated with the serum-added standard curve was almost equal to the actual micafungin serum concentration (the ratio of antifungal activity estimated by the disk diffusion method based on the serum-free standard curve to that measured by HPLC was 89% ± 23% [mean ± standard deviation, ranging from 58% to 135%]) (Table 2).

MIC for micafungin against *C. albicans* FP633 in heat-inactivated serum from a volunteer was 1 μg/ml, which was consistent with previously reported data using the same strain (3). At this concentration, micafungin induced swelling and subsequent burst of mycelia. Inhibitory titers for serum samples from all patients are summarized in Table 2. Representative results from patient no. 5 are shown in Fig. 2. These titers were in excellent agreement with both micafungin concentrations in serum samples by HPLC and those estimated from the serum-added standard curve (Table 2).

These results indicate that serum proteins certainly bind to micafungin and reduce its antifungal activity, but this binding may be reversible and weak. These data are inconsistent with the free-drug hypothesis. One or more of the following reasons could explain this discrepancy. First, micafungin binds to serum proteins at 99.8% in situations without any other competitors, such as in ultrafiltration, the method measuring the equilibrium binding (13). If fungi susceptible to micafungin are present, however, micafungin may be easily released from the protein-bound form in a rapid equilibrium, bind to target pathogens, and exert its antifungal activity. In this case, increased MIC of micafungin in serum may depend on the fungal strains being tested (6, 7). Furthermore, although albumin is supposed to bind mainly to micafungin, several other proteins in serum, such as alpha and gamma globulins, might influence the interactions among micafungin, serum proteins, and target pathogens (8).

In conclusion, it seems to be unsuitable to apply the free-drug hypothesis to the pharmacodynamics of micafungin, because this may underestimate its antifungal activity. We have shown, using the disk diffusion and broth dilution methods, that serum samples from micafungin-treated patients exhibited adequate antifungal activity. Our data will be useful for understanding the pharmacodynamics of micafungin and for improving the clinical outcome of micafungin treatment.

This study was supported in part by a grant from Astellas Pharma Inc.

REFERENCES

1. **Ascioglu, S., J. H. Rex, B. de Pauw, J. E. Bennett, J. Bille, F. Crokaert, D. W. Denning, J. P. Donnelly, J. E. Edwards, Z. Erjavec, D. Fiere, O. Lortholary, J. Maertens, J. F. Meis, T. F. Patterson, J. Ritter, D. Selleslag, P. M. Shah, D. A. Stevens, and T. J. Walsh, the Invasive Fungal Infections Cooperating Group of the European Organization for Research and Treatment of Cancer, and Mycoses Study Group of the National Institute of Allergy and Infectious Diseases.** 2002. Defining opportunistic invasive fungal infections in immunocompromised patients with cancer and hematopoietic stem cell transplants: an international consensus. Clin. Infect. Dis. **34**:7–14.
2. **Azuma, J., K. Nakahara, A. Kagayama, T. Kajiho, A. Kawamura, H. Suematsu, and T. Mukai.** 2002. Phase I study of micafungin. Jpn. J. Chemother. **50**(Suppl. 1):104–147.
3. **Maki, K., S. Matsumoto, E. Watabe, Y. Iguchi, M. Tomishima, H. Ohki, A. Yamada, F. Ikeda, S. Tawara, and S. Mutoh.** 2008. Use of a serum-based antifungal susceptibility assay to predict the in vivo efficacy of novel echinocandin compounds. Microbiol. Immunol. **52**:383–391.
4. **National Committee for Clinical Laboratory Standards.** 2002. Reference method for broth dilution antifungal susceptibility testing of yeast. Approved standard M27-A2. NCCLS, Wayne, PA.
5. **National Committee for Clinical Laboratory Standards.** 2004. Method for antifungal disc diffusion susceptibility testing of yeasts: proposed guideline M44-A. NCCLS, Wayne, PA.

6. **Odabasi, Z., V. Paetznick, J. H. Rex, and L. Ostrosky-Zeichner.** 2007. Effects of serum on in vitro susceptibility testing of echinocandins. Antimicrob. Agents Chemother. **51**:4214–4216.
7. **Paderu, P., G. Garcia-Effron, S. Balashov, G. Delmas, S. Park, and S. Perlin.** 2007. Serum differentially alters the antifungal properties of echinocandin drugs. Antimicrob. Agents Chemother. **51**:2253–2256.
8. **Schäfer-Korting, M., H. C. Korting, W. Rittler, and W. Obermüller.** 1995. Influence of serum protein binding on the in vitro activity of antifungal agents. Infection **23**:292–297.
9. **Tabata, K., M. Katashima, A. Kawamura, Y. Tanigawara, and K. Sunagawa.** 2006. Linear pharmacokinetics of micafungin and its active metabolites in Japanese pediatric patients with fungal infections. Biol. Pharm. Bull. **29**:1706–1711.
10. **Tamura, K., A. Urabe, M. Yoshida, A. Kanamaru, Y. Kodera, S. Okamoto, S. Maesaki, and T. Masaoka.** 2008. Efficacy and safety of micafungin, an echinocandin antifungal agent, on invasive fungal infections in patients with hematological disorders. Leuk. Lymphoma **50**:92–100.
11. **Tawara, S., F. Ikeda, K. Maki, Y. Morishita, K. Otomo, N. Teratani, T. Goto, M. Tomishima, H. Ohki, A. Yamada, K. Kawabata, H. Takasugi, K. Sakane, H. Tanaka, F. Matsumoto, and S. Kuwahara.** 2000. In vitro activities of a new lipopeptide antifungal agent, FK463, against a variety of clinically important fungi. Antimicrob. Agents Chemother. **44**:57–62.
12. **Yamato, Y., H. Kaneko, K. Tanimoto, M. Katashimaet, K. Ishibashi, A. Kamamura, M. Terakawa, and A. Kagayama.** 2002. Simultaneous determination of antifungal drug, micafungin, and its two active metabolites in human plasma using high-performance liquid chromatography with fluorescence detection. Jpn. J. Chemother. **50**(Suppl. 1):68–73.
13. **Yamato, Y., H. Kaneko, T. Hashimoto, M. Katashima, K. Ishibashi, A. Kawamura, M. Terakawa, and A. Kagayama.** 2002. Pharmacokinetics of the antifungal drug micafungin in mice, rats and dogs, and its in vitro protein binding and distribution to blood cells. Jpn. J. Chemother. **50**(Suppl. 1):74–79.

Journal of Thrombosis and Haemostasis, 7: 1373–1383 DOI: 10.1111/j.1538-7836.2009.03510.x

ORIGINAL ARTICLE

Presence of platelet-associated anti-glycoprotein (GP)VI autoantibodies and restoration of GPVI expression in patients with GPVI deficiency

M. AKIYAMA,* H. KASHIWAGI,* K. TODO,† M. MOROI,‡ M. C. BERNDT,§ H. KOJIMA,¶ Y. KANAKURA* and Y. TOMIYAMA*††

**Department of Haematology and Oncology, Graduate School of Medicine C9, Osaka University, Osaka; †Department of Paediatrics, Kyoto Second Red Cross Hospital, Kyoto; ‡Department of Protein Biochemistry, Institute of Life Science, Kurume University, Fukuoka, Japan; §College of Medicine and Health, University College Cork, Cork, Ireland; ¶Department of Haematology and Oncology, Ibaraki Prefectural Central Hospital, Ibaraki; and ††Department of Blood Transfusion, Osaka University Hospital, Osaka, Japan*

To cite this article: Akiyama M, Kashiwagi H, Todo K, Moroi M, Berndt MC, Kojima H, Kanakura Y, Tomiyama Y. Presence of platelet-associated anti-glycoprotein (GP)VI autoantibodies and restoration of GPVI expression in patients with GPVI deficiency. *J Thromb Haemost* 2009; 7: 1373–83.

Summary. *Background:* Glycoprotein (GP)VI deficiency is a rare platelet disorder with a mild bleeding tendency. However, its pathophysiology remains unclear. *Objectives:* We characterized a novel GPVI-deficient patient with immune thrombocytopenic purpura and searched for the presence of anti-GPVI autoantibodies in this and another patient with GPVI deficiency. *Methods and results:* A 12-year-old Japanese girl (case 1) with moderate thrombocytopenia and mild bleeding showed selectively impaired collagen-induced platelet aggregation. Flow cytometric analysis indicated that the patient had a defect in the expression of GPVI–FcRγ. An eluate of her platelet-associated IgG contained anti-$\alpha_{IIb}\beta_3$ autoantibodies. Moreover, using GPVI–FcRγ-transfected cells, we unexpectedly identified anti-GPVI antibodies against the soluble ectodomain of GPVI in the eluate, despite the patient's GPVI deficiency. In contrast, anti-GPVI antibodies were not detectable in her plasma. In another case of GPVI deficiency (case 2) without detectable plasma anti-GPVI antibodies, we again detected platelet-associated anti-GPVI antibodies. In a 2-year follow-up of case 1, the platelet count increased to within the normal range and the bleeding tendency improved. Interestingly, GPVI was again expressed on her platelets, in association with a decrease in the relative amount of anti-GPVI antibodies. *Conclusions:* This is the first demonstration of platelet-associated anti-GPVI antibodies in GPVI-deficient subjects, in one case with spontaneous restoration of GPVI expression. These results strongly suggest an autoimmune mechanism in GPVI deficiency.

Keywords: GPVI deficiency, immune thrombocytopenic purpura, platelet-associated autoantibody.

Introduction

Glycoprotein (GP)VI is a 62-kDa transmembrane protein that plays a key role in platelet adhesion to collagen and subsequent platelet activation. GPVI consists of two immunoglobulin-like domains, a short mucin-like domain, a transmembrane domain, and a 51 amino acid cytoplasmic domain. GPVI is non-covalently associated with the immunoreceptor tyrosine-based activation motif (ITAM)-containing FcRγ-chain in the platelet membrane. Ligand binding to the GPVI–FcRγ-chain complex induces signals via the Syk/SLP-76/PLCγ2 pathway to activate integrins $\alpha_2\beta_1$ (also known as GPIa–IIa) and $\alpha_{IIb}\beta_3$ (GPIIb–IIIa), leading to thrombus formation [1–3].

GPVI deficiency is a rare platelet disorder with a mild bleeding tendency. Twelve cases have been reported to date since the first Japanese case in 1987 [4–15]. Although preliminary reports showed molecular defects in the GPVI gene in two cases of congenital GPVI deficiency [13,14], an immunologic mechanism has been suggested as the more frequent etiology for the depletion of GPVI [16]. In fact, plasma anti-GPVI antibodies have been demonstrated in five patients with GPVI deficiency [4,8,10,12,15], and injection of anti-GPVI monoclonal antibodies such as JAQ1 induces the selective downregulation of GPVI from platelets in mice [17,18] and monkeys [19]. Human GPVI can also be downregulated in a NOD/SCID mouse model by injection of human platelets and an anti-GPVI antibody [20]. Recent reports suggest that GPVI downregulation by anti-GPVI antibodies occurs through metalloprotease-mediated ectodomain shedding and/

Correspondence: Yoshiaki Tomiyama, Department of Blood Transfusion, Osaka University Hospital, 2-15 Yamadaoka, Suita Osaka 565-0871, Japan.
Tel.: +81 6 6879 5887; fax: +81 6 6879 5889.
E-mail: yoshi@hp-blood.med.osaka-u.ac.jp

Received 9 December 2008, accepted 27 April 2009

or internalization/degradation pathways [18,19]. However, the pathophysiologic cause of GPVI deficiency in humans still remains unclear, because no anti-GPVI antibodies were demonstrated in the remaining five cases.

In this study, we have characterized a novel case of GPVI deficiency (case 1) and demonstrated the presence of platelet-associated anti-GPVI autoantibodies despite GPVI deficiency. Similar findings were obtained in a previously described patient with unknown etiology (case 2) [11]. Moreover, in a 2-year follow-up of case 1, we observed the spontaneous restoration of GPVI expression with a reduction in platelet-associated anti-GPVI antibodies, indicating that GPVI deficiency in our patient was an acquired abnormality. Our present data provide new evidence for an autoimmune mechanism in the pathophysiology of GPVI deficiency.

Materials and methods

Reagents

Mouse monoclonal anti-GPVI antibody 204-11 and rabbit polyclonal anti-GPVI cytoplasmic tail antibody have been described previously [21,22]. Biotinylated convulxin was made as previously described [23]. 293 cells stably expressing $\alpha_{IIb}\beta_3$ were established as previously described [24]. Chinese hamster ovary (CHO) cells stably expressing GPVI and FcRγ-chain (GPVI–FcRγ CHO cells) and the soluble form of recombinant human GPVI (amino acids 24–219; rhGPVI) were generously provided by J. Kambayashi (Otsuka USA) [25]. Rabbit polyclonal anti-FcRγ antibody and goat polyconal anti-FcγRIIA antibody were obtained from Upstate Biotechnology (Lake Placid, NY, USA) and R&D Systems (Minneapolis, MN, USA), respectively. Mouse monoclonal anti-α_2 antibody Gi9 and anti-β_3 antibody VL-PL2 were obtained from Immunotech International (Marseille, France) and BD Pharmingen (San Jose, CA, USA), respectively.

Platelets, mononuclear cells, and platelet-associated IgG eluate preparation

This study was approved by the Institutional Review Board at Osaka University Hospital, and blood samples were obtained with written informed consent. Platelets were obtained by differential centrifugation from blood anticoagulated with either Na_2-EDTA or sodium citrate [26]. Mononuclear cells were obtained using a Ficoll–Paque gradient [27]. Platelet-associated antibodies were eluted from washed platelet suspensions at a concentration of $200 \times 10^3\ \mu L^{-1}$ by adding an equal amount of diethyl ether as previously described [26,28].

Platelet aggregation study

Platelets in platelet-rich plasma were stimulated with various agonists, and platelet aggregation was monitored using a model PAM-6C platelet aggregometer (Mebanix, Tokyo, Japan).

Flow cytometry

Platelet-associated IgG and surface expression of platelet GPs were analyzed by flow cytometry as previously described [28,29]. In the case of the 204-11 anti-GPVI monoclonal antibody, prostaglandin E_1 was always added to the platelet suspension to prevent aggregation. Specific binding of 204-11 was calculated by subtraction of mean fluorescence intensity (MFI) of the control from that of 204-11, and relative surface expression was estimated by comparison of the specific binding of 204-11 of the patients' platelets with that of normal platelets. To detect autoantibodies in eluates, GPVI–FcRγ CHO cells and $\alpha_{IIb}\beta_3$-expressing 293 cells were used. Cells were suspended in phosphate-buffered saline (PBS) at a concentration of $5 \times 10^6\ \mu L^{-1}$. Fifty-microliter aliquots of the eluates were incubated with an equal volume of cell suspension for 30 min on ice, and this was followed by incubation with Alexa488-conjugated anti-human IgG (Molecular Probes, Eugene, OR, USA) for 20 min. In the case of GPVI–FcRγ CHO cells, the cells were incubated simultaneously with 10 μg mL^{-1} 204-11 and with phycoerythrin-conjugated anti-mouse $F(ab')_2$ antibody (Serotec, Oxford, UK) to monitor the expression of GPVI. After washing, the cells were suspended in propidium iodide-containing PBS, and multicolor flow cytometric analysis was performed.

For the detection of anti-GPVI antibodies in plasma, platelet-poor plasma was incubated with wild-type CHO cells for 1 h to remove non-specific binding, and then incubated with GPVI–FcRγ CHO cells.

Western blotting

Western blotting was performed as previously described [30]. Twenty-microgram aliquots of platelet lysates were electrophoresed on 5–20% gradient sodium dodecylsulfate polyacrylamide gel electrophoresis gels (Pagel; ATTO korp, Tokyo, Japan) under non-reducing conditions for 204-11 and biotinylated convulxin binding, and under reducing conditions for the anti-GPVI cytoplasmic tail antibody. After transfer to poly(vinylidene difluoride) membranes (Immobilon; Millipore, Bedford, MA, USA), the membranes were incubated with either antibody or convulxin, and then incubated with the appropriate horseradish peroxidase (HRP)-conjugated secondary antibody or HRP-conjugated streptoavidin (Vectastain ABC Kit; Vector Laboratories, Burlingame, CA, USA). The optical density of the bands was measured using Scion Image software (Scion Corp., Frederick, MD, USA).

N-ethylmaleimide (NEM) treatment of platelets

NEM treatment of platelets was performed as previously described [31]. In brief, $500 \times 10^3\ \mu L^{-1}$ of washed platelets were incubated with 2 mM NEM (Calbiochem, La Jolla, CA, USA) for 15 min at room temperature, and the reaction was terminated by addition of an equal amount of 10 mM EDTA/PBS.

Competition assay for 204-11 binding to rhGPVI by anti-GPVI autoantibodies

Two hundred and fifty nanograms of rhGPVI was coated per microtiter well. After blocking with bovine serum albumin (BSA), 50-μL aliquots of the patient's platelet eluates were added to each well and incubated for 1 h at room temperature. After washing, 1 μg mL^{-1} of 204-11 or MOPC was added to each well and incubated for another 1 h at room temperature, and this was followed by incubation with alkaline phosphatase-conjugated anti-mouse IgG (Sigma, St. Louis, MO, USA). Alkaline phosphatase activity was measured using disodium phenylphosphate as substrate (Sanko Jun-yaku, Tokyo, Japan).

Dot blot analysis

One hundred nanograms of rhGPVI was dotted onto a nitrocellulose membrane. After blocking with BSA, the membrane was incubated with the patient's platelet eluates for 1 h. The binding of anti-GPVI antibodies was detected by incubation with biotinylated anti-human IgG (Jackson ImmunoResearch Laboratories, West Grove, PA, USA), and this was followed by incubation with HRP-conjugated streptoavidin and a chemiluminescence reaction. As a control for blotting of rhGPVI, biotinylated convulxin was incubated with the membrane, and this was followed by incubation with HRP-conjugated streptoavidin.

RNA preparation, reverse transcription polymerase chain reaction (RT-PCR), and sequence analysis

Platelet RNA was extracted using Trizol solution (Invitrogen, Carlsbad, CA, USA) according to the manufacturer's instructions. RT-PCR and direct sequencing were performed as previously described [29]. Sequences for the primers were as described previously [11].

Results

Cases

Case 1 A 12-year-old Japanese girl suffering from cutaneous ecchymosis and recurrent epistaxis since May 2006 was referred to Osaka University Hospital in August 2006. There was no family history of a bleeding tendency or consanguinity. Physical examination revealed several petechiae in the upper and lower limbs and chest. Her platelet count was 133×10^3 μL^{-1}, with normal white blood cell and red blood cell counts. There were no abnormalities in blood chemistry and coagulation. Her platelet count decreased to $\sim 80 \times 10^3$ μL^{-1} in the next 2 months. It recovered spontaneously, but remained consistently low, ranging from 100×10^3 μL^{-1} to 120×10^3 μL^{-1} over a 12-month period. The bleeding tendency was unchanged in this period. However, after February 2008, the platelet count increased to more than 150×10^3 μL^{-1}, with improvement of the bleeding tendency (Fig. 1A).

Case 2 A 31-year-old Japanese GPVI-deficient female without any detectable anti-GPVI antibodies or genetic aberrations has been described previously [11].

Platelet aggregation study

The case 1 patient had a prolonged bleeding time (> 10 min, Duke's method), despite a platelet count of more than 100×10^3 μL^{-1} in November 2006, suggesting that functional abnormalities may exist in the patient's platelets. Collagen-induced platelet aggregation was markedly impaired in the patient (Fig. 1B). Although epinephrine-induced aggregation was impaired, impairment is observed in ~ 16% of Japanese healthy controls and is not associated with a bleeding diathesis [32]. The impaired collagen-induced platelet aggregation was not corrected even at 10 μg mL^{-1} collagen, although modest concentration-dependent aggregation was observed (Fig. 1B). These data suggest that the patient possessed a defect in a platelet collagen receptor.

Expression of GPVI and FcRγ

GPVI and $\alpha_2\beta_1$ are known to be the two major collagen receptors on platelets [1–3]. Flow cytometric analysis using an anti-GPVI monoclonal antibody, 204-11, indicated that surface GPVI expression was markedly reduced (3% of control) on the patient's platelets, whereas the expression levels of $\alpha_2\beta_1$, GPIb, $\alpha_{IIb}\beta_3$ and CD36 (data not shown) were normal (Fig. 2A). No reduction in GPVI expression was observed on platelets obtained from the patient's mother or the elder sister. Next, we examined binding of convulxin, 204-11 and a polyclonal anti-GPVI cytoplasmic tail antibody to platelet lysates in an immunoblot assay. Biotinylated convulxin binding was markedly reduced, reflecting the result obtained for GPVI expression by flow cytometry (< 5% of control) (Fig. 2B). Binding of 204-11 was also greatly reduced (~ 5% of normal control Fig. 2C). In contrast, anti-GPVI cytoplasmic tail antibody revealed that the patient platelet lysate contained a significant amount (14% of control) of normal-sized GPVI (Fig. 2D,E). It is known that GPVI is shed near the transmembrane domain by a metalloprotease after binding its ligands such as collagen or by anti-GPVI antibodies, resulting in production of an ~ 55-kDa soluble ectodomain fragment and an ~ 10-kDa platelet-associated remnant fragment [31]. Treatment of platelets with a metalloprotease activator, NEM, also induces the same effects (Fig. 3F) [31]. However, we could not detect any remnant GPVI fragment in the patient platelet lysate (Fig. 2D). In addition, we confirmed that there were no abnormalities, at least in the coding region of GPVI cDNA obtained from the patient's platelets, except for the common polymorphism

Gln317 → Leu as homozygote by direct sequencing analysis (data not shown) [33].

FcRγ expression in platelets from the case 1 patient was markedly reduced, whereas FcRγ expression was normal in the patient's mononuclear cells (Fig. 2F). We confirmed that there were no sequence abnormalities in the coding region of FcRγ cDNA obtained from the patient's platelets (data not shown). In addition, we detected normal expression of FcγRIIA in platelets from the case 1 patient (Fig. 2F).

Detection and analysis of platelet-associated anti-GPVI antibodies

As the case 1 patient's platelets possessed an elevated level of platelet-associated IgG (PAIgG) (MFI 42.44; Fig. 3A), we eluted antibodies from the platelets using diethyl ether. We confirmed that the eluted antibodies had the ability to bind to control platelets (data not shown). We detected anti-$\alpha_{IIb}\beta_3$ antibodies in the eluate by employing $\alpha_{IIb}\beta_3$-transfected 293 cells (Fig. 3B). We then used GPVI–FcRγ CHO cells to search for the presence of anti-GPVI antibodies. We monitored the expression of GPVI with 204-11, and two-color flow cytometric analysis was performed because of heterogeneity in the expression of GPVI. We used eluates obtained from normal controls and an immune thrombocytopenic purpura (ITP) patient with elevated PAIgG (MFI 43.87) as negative controls. As shown in Fig. 3C, antibody binding depending on the expression of GPVI was clearly observed in the eluate of case 1. To exclude the possibility of cross-reactivity of the anti-$\alpha_{IIb}\beta_3$ antibodies with the GPVI–FcRγ CHO cells, anti-$\alpha_{IIb}\beta_3$ antibodies in the eluate were precleared by incubation with $\alpha_{IIb}\beta_3$-transfected 293 cells, and then IgG antibody binding was reanalyzed. Antibody binding to the GPVI–FcRγ CHO cells was not affected by the depletion of the $\alpha_{IIb}\beta_3$ antibodies (data not shown). These data clearly demonstrate the presence of platelet-associated autoantibodies specific for GPVI in case 1. Moreover, preclearing the eluate with $\alpha_{IIb}\beta_3$-transfected 293 cells and with $\alpha_{IIb}\beta_3$-transfected 293 cells plus GPVI–FcRγ CHO cells decreased IgG binding to control platelets by 45% and by 87%, respectively. These results indicate that the PAIgG of the patient is mainly composed of anti-GPIIb–IIIa and anti-GPVI antibodies (data not shown).

To localize the epitope(s) for the anti-GPVI antibodies, we next examined the binding of the anti-GPVI antibodies to

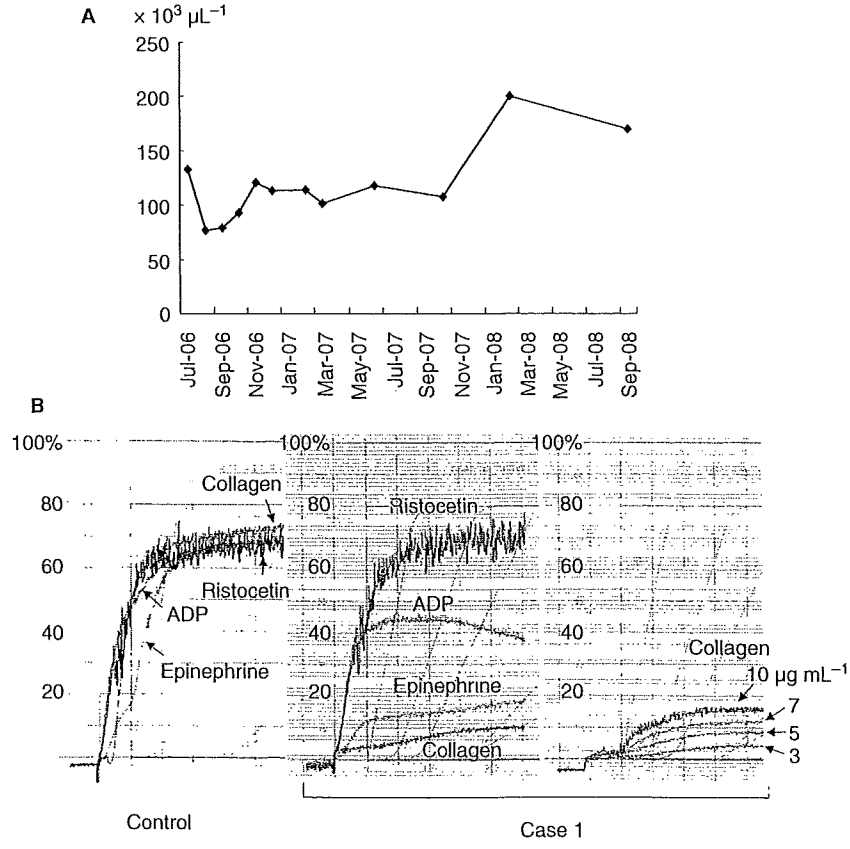

Fig. 1. Platelet counts and platelet aggregation study of the case 1 patient. (A) Time course of the platelet count for the case 1 patient from July 2006 to September 2008. (B) Platelet-rich plasma obtained from a normal control (left panel) or the patient (case 1) in November 2006 (middle panel) was stimulated with ADP (2.0 μM), ristocetin (1.5 mg mL^{-1}), epinephrine (2.0 μM), or collagen (3.0 μg mL^{-1}). Platelet-rich plasma from case 1 was stimulated with collagen at the indicated concentrations (3.0–10.0 μg mL^{-1}) (right panel).

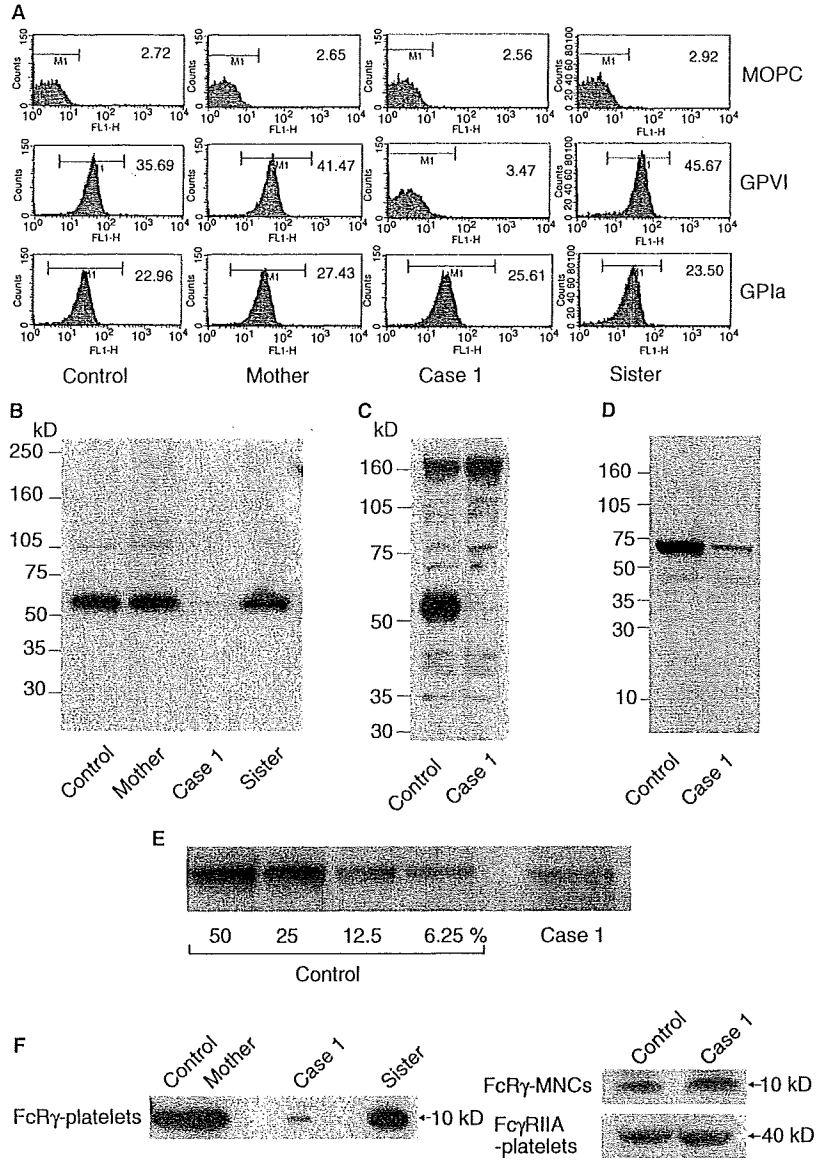

Fig. 2. Expression of glycoprotein (GP)VI and FcRγ in the case 1 patient. (A) Flow cytometric analysis of patient platelets (case 1). Platelets obtained in November 2006 from a control, the patient's mother, the patient (case 1) and an elder sister were incubated with either a monoclonal anti-GPVI antibody, 204-11, a monoclonal anti-α_2 antibody, Gi9, or a control IgG, MOPC, and analyzed by flow cytometry. Numbers in each histogram represent the mean fluorescence intensity of the gated cells. (B) Platelet lysates (20 μg) obtained from the control, the mother, the patient (case 1) and the sister were electrophoresed on a sodium dodecylsulfate polyacrylamide gel electrophoresis (SDS-PAGE) gel under non-reducing conditions. After transfer to poly(vinylidene difluoride) membranes, the membranes were incubated with biotinylated convulxin, followed by horseradish peroxidase-conjugated avidin. (C) Platelet lysates (20 μg) were electrophoresed on an SDS-PAGE gel under non-reducing conditions, and this was followed by blotting with 204-11. (D) Platelet lysates (20 μg) were electrophoresed on an SDS-PAGE gel under reducing conditions, and this was followed by blotting with polyclonal anti-GPVI cytoplasmic tail antibody. (E) Quantification of GPVI in platelet lysates of case 1. Serially diluted control lysates and the patient's lysate were electrophoresed on an SDS-PAGE gel and detected by polyclonal anti-GPVI cytoplasmic tail antibody. (F) Left panel: platelet lysates were electrophoresed under reducing conditions, and FcRγ expression was analyzed using an anti-FcRγ polyclonal antibody. Right panel: mononuclear cell (MNC) lysates (upper) or platelet lysates (lower) were electrophoresed under reducing conditions, and FcRγ expression in mononuclear cells and FcγRIIA expression in platelets were examined using anti-FcRγ and anti-FcγRIIA polyclonal antibodies, respectively.

rhGPVI (amino acids 24–219). With dot blot analysis, antibody binding to rhGPVI was clearly detected in the patient's platelet eluate (Fig. 3D). We then investigated whether the epitope for 204-11 and the anti-GPVI autoantibodies might be close to each other. As shown in Fig. 3E, the eluate obtained from case 1 did not inhibit 204-11 binding to immobilized rhGPVI. Preincubation of GPVI–FcRγ CHO cells with 204-11 also did not inhibit anti-GPVI autoantibody binding to the cells (data not shown). NEM treatment led to complete loss of the ectodomain of GPVI, whereas significant amounts of an

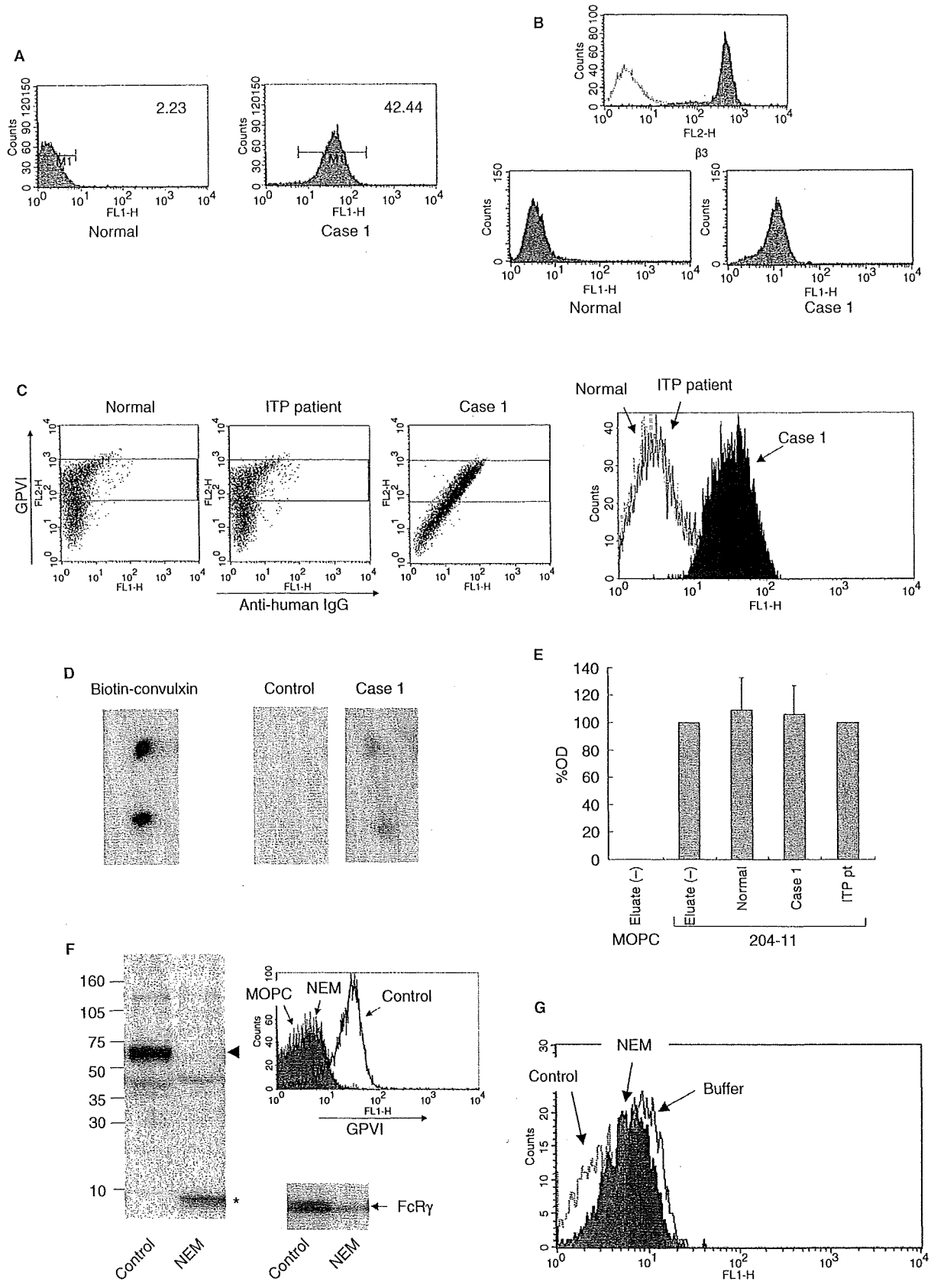

Fig. 3. Detection and analysis of platelet-associated anti-glycoprotein (GP)VI antibodies in the case 1 patient. (A) Elevated platelet-associated IgG (PAIgG) in the patient (case 1). Platelets obtained from the patient in November 2006 showed elevated PAIgG levels. The number in the histogram indicates mean fluorescence intensity (MFI) of the gated region. (B) Upper panel: the binding of anti-β_3 monoclonal antibody, VI-PL2 (shaded) or MOPC (open) to $\alpha_{IIb}\beta_3$-expressing 293 cells is shown. Lower panel: platelet-associated antibodies were eluted with diethyl ether, and IgG binding in the eluates was examined using $\alpha_{IIb}\beta_3$-expressing 293 cells. (C) Detection of platelet-associated anti-GPVI antibodies in the patient (case 1). Left panels: platelet eluates obtained from a normal control, an immune thrombocytopenic purpura (ITP) patient who had elevated PAIgG (MFI 43.87) or case 1 were incubated with GPVI–FcRγ Chinese hamster ovary (CHO) cells, followed by Alexa488-conjugated anti-human IgG. GPVI expression was monitored by incubation with 204-11, followed by phycoerythrin-conjugated anti-mouse IgG. Right panel: binding of human IgG to the cells expressing high levels of GPVI (gated area in the dot blots) was examined and expressed as a histogram (open dotted line for control subject, open solid line for ITP patient, and shaded histogram for case 1). (D) One hundred nanograms of recombinant human GPVI (rhGPVI) was dotted onto a nitrocellulose membrane in duplicate and incubated with platelet eluate from the patient. IgG binding to rhGPVI was detected with biotinylated anti-human IgG, followed by horseradish peroxidase (HRP)-conjugated streptoavidin. The left panel shows the binding of biotinylated convulxin as a positive control. (E) Two hundred and fifty nanograms of rhGPVI was coated on each well of a microtiter plate. Fifty microliters of eluate or buffer was added to each well and incubated for 1 h. After washing, 1 μg mL^{-1} 204-11 or MOPC was added to each well and incubated for another 1 h, and this was followed by incubation with alkaline phosphatase-conjugated anti-mouse IgG. Alkaline phosphatase activity was measured using disodium phenylphosphate as a substrate. Relative optical density (OD) against buffer is indicated as mean + standard deviation of three independent experiments. (F) *N*-ethylmaleimide (NEM) treatment of platelets. Platelets were treated with 2 mM NEM for 15 min at room temperature. GPVI expression of the NEM-treated platelets was analyzed by fluorescence-activated cell sorting analysis with 204-11 (right upper panel), and immunoblotting with anti-GPVI cytoplasmic tail antibody (left panel) or anti-FcRγ polyclonal antibody (right lower panel). ◀, full-length GPVI; *, ~ 10-kDa platelet-associated remnant fragment of GPVI. Note that the NEM treatment led to complete loss of the ectodomain of GPVI in platelets, whereas significant amounts of the remnant fragment of GPVI and FcRγ remained platelet-associated. (G) Platelet eluates were preincubated with NEM-treated platelets (NEM: shaded) or control platelets (control: open, dotted line), or diluted with the same amount of buffer (buffer: open, solid line), and IgG binding to CHO cells expressing high levels of GPVI was then analyzed. In contrast to the preincubation with control platelets, preincubation with NEM-treated platelets failed to significantly inhibit IgG binding to CHO cells expressing high levels of GPVI.

~ 10-kDa platelet-associated remnant GPVI fragment and FcRγ remained on NEM-treated platelets (Fig. 3F). Absorption of the eluate with the NEM-treated platelets did not show a significant decrease in the binding of anti-GPVI antibodies to GPVI–FcRγ CHO cells (Fig. 3G). These results indicate that the anti-GPVI antibodies in case 1 did not recognize epitope(s) on the remnant 10-kDa GPVI fragment or FcRγ chain, but mainly recognized epitope(s) on the extracellular domain of GPVI, which is (are) apparently different from the 204-11 epitope.

Detection of anti-GPVI antibodies in plasma

We next tried to detect anti-GPVI antibodies in the plasma from the case 1 patient. We first examined whether the patient's plasma could induce platelet aggregation. However, addition of 20% of the patient's plasma to normal platelet-rich plasma did not induce platelet aggregation or inhibition of collagen-induced aggregation (Fig. 4A). We also failed to detect plasma anti-GPVI antibodies with the use of GPVI–FcRγ CHO cells (Fig. 4B). Although this experiment suggested that collagen-induced platelet aggregation may be increased in the presence of the patient's plasma as compared with control and the mother's plasma, this characteristic was not reproducible in additional experiments (data not shown). These results indicate that there were no detectable anti-GPVI antibodies in the patient's plasma.

Detection of platelet-associated anti-GPVI autoantibodies in a second GPVI-deficient patient (case 2)

We also searched for the presence of platelet-associated anti-GPVI autoantibodies in the case 2 GPVI-deficient patient. Like the case 1 patient, she had suffered ITP, but no plasma anti-GPVI autoantibodies were detected, despite intensive analysis [11]. We confirmed that GPVI expression on the case 2 patient's

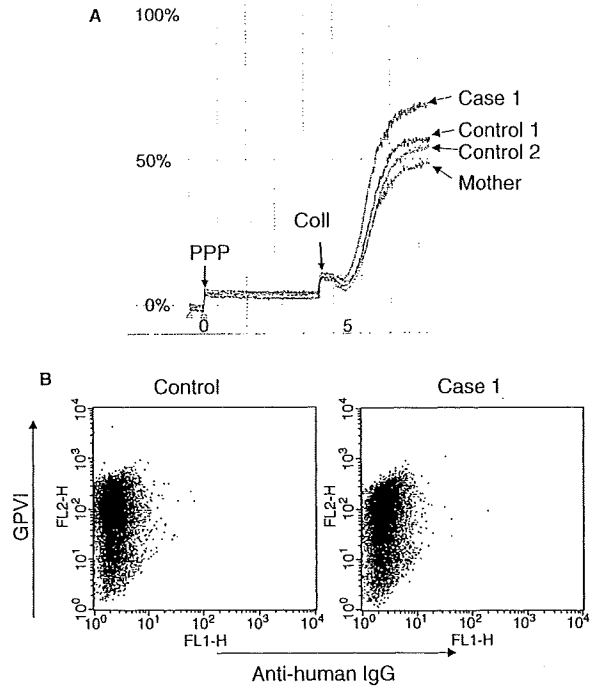

Fig. 4. Detection of anti-glycoprotein (GP)VI antibodies in plasma from the case 1 patient. (A) Effects of the patient's (case 1) plasma on control platelet function. Twenty-four microliters of platelet-poor plasma (PPP) obtained from case 1, the mother and two normal controls was added to 96 μL of platelet-rich plasma obtained from a control. After 4 min of incubation, 1 μg mL^{-1} collagen (Coll) was added. (B) Platelet-poor plasma from the patient was preincubated with wild-type Chinese hamster ovary (CHO) cells for 1 h to remove non-specific binding, and then incubated with GPVI–FcRγ CHO cells. Binding of human IgG to CHO cells expressing high levels of GPVI was analyzed as described in Fig. 3C.

platelets was still markedly impaired over a 5-year follow-up after the initial diagnosis in 2003 (Fig. 5A,B). The expression level of GPVI was much lower than that of the case 1 patient.

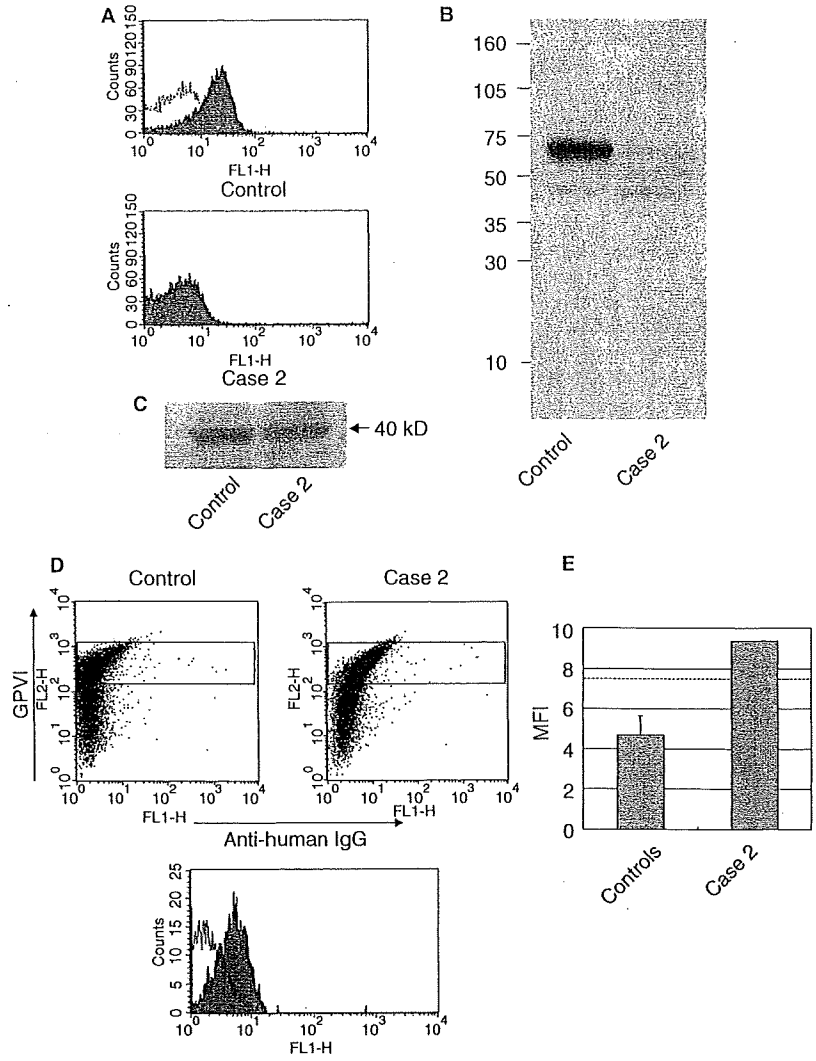

Fig. 5. Detection of platelet-associated anti-glycoprotein (GP)VI antibodies in the case 2 patient. (A) Flow cytometric analysis of platelets obtained from a control or the patient (case 2) with 204-11 (shaded) or MOPC (open). (B) Immunoblotting of platelet lysate obtained from a control or the patient (case 2) with polyclonal anti-GPVI cytoplasmic tail antibody. (C) FcγRIIA expression in platelets obtained from a control and the patient (case 2). (D) Detection of platelet-associated anti-GPVI antibodies in the patient (case 2). Binding of human IgG to the cells expressing high levels of GPVI (the gated area in the dot blots) was examined and expressed as a histogram (open histogram for control subject, shaded histogram for the patient, case 2). (E) Mean fluorescence intensity (MFI) for five control subjects (4.70 ± 0.94; mean ± standard deviation) from Fig. 5D and MFI for the patient (case 2) (9.35) are shown. The dotted line represents mean + 3 standard deviations (7.53) of control subjects.

Again, we could not detect any ~ 10-kDa remnant fragment of GPVI in the case 2 platelet lysate (Fig. 5B), but detected normal FcγRIIA expression (Fig. 5C). PAIgG was slightly elevated (data not shown). In the eluate obtained from the patient's platelets, we detected low but significant antibody binding to GPVI–FcRγ CHO cells (Fig. 5D,E).

Restoration of collagen-induced platelet aggregation and GPVI expression in the case 1 patient

In February 2008, the platelet count of the case 1 patient increased to $200 \times 10^3\ \mu L^{-1}$ and the bleeding tendency improved (Fig. 1A). As shown in Fig. 6A, the platelet response to collagen was still impaired, but was clearly improved as compared with that in November 2006 (see Fig. 1B). Flow cytometric analysis with 204-11 revealed that surface expression levels of GPVI on the patient's platelets were restored to 9% and 40% of control in February 2008 and September 2008, respectively (Fig. 6B). Comparable results were obtained by western blotting using anti-GPVI tail antibodies (12% and 38% in February and September 2008, respectively; Fig. 6C). Anti-GPVI autoantibodies were still detectable in eluates obtained from patient's platelets in February and September 2008, but the amounts of the antibodies relative to GPVI expression levels were markedly decreased in September 2008 (Fig. 6D). The amounts of anti-$\alpha_{IIb}\beta_3$ autoantibodies in the eluates of February and September 2008 were also markedly decreased (Fig. 6E).

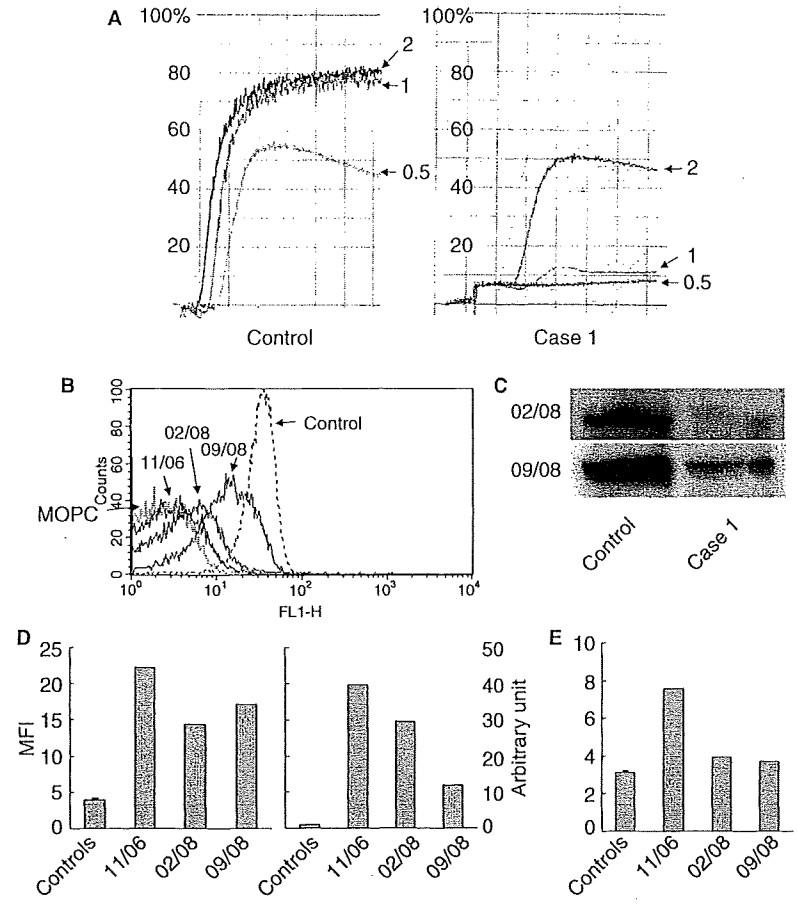

Fig. 6. Transition of platelet aggregation, glycoprotein (GP)VI expression and anti-GPVI antibodies in the case 1 patient. (A) Collagen-induced platelet aggregation in the patient (case 1) in February 2008. Platelet aggregation of a control and of case 1 with the indicated concentration of collagen are shown. Note that the patient's platelets showed clear aggregation induced by 2 μg mL^{-1} collagen (compare with Fig. 1B). (B) Surface GPVI expression in case 1 platelets obtained in November 2006 (06/11), February (08/02) and September 2008 (08/09) was analyzed by flow cytometry with 204-11. (C) GPVI expression in platelet lysates obtained in February and September 2008 was analyzed by western blotting with the anti-GPVI cytoplasmic tail antibody. (D) Anti-GPVI antibodies in eluates obtained on 06/11, 08/02 and 08/09 were analyzed using GPVI–FcRγ Chinese hamster ovary (CHO) cells as described in Fig. 3C. Left panel: mean fluorescence intensity (MFI) for antibody binding with CHO cells expressing high levels of GPVI is shown. Right panel: the amounts of anti-GPVI antibodies relative to GPVI expression levels. The MFI for the GPVI antibodies was divided by the GPVI expression levels estimated by immunoblotting at each indicated date. Data are expressed as the ratio to a normal control, which is defined as one arbitrary unit. (E) Anti-$\alpha_{IIb}\beta_3$ antibodies in eluates were analyzed as described in Fig. 3B, and the MFI is shown.

Discussion

In this article, we have demonstrated for the first time the presence of platelet-associated anti-GPVI autoantibodies in two GPVI-deficient patients with no detectable plasma anti-GPVI antibodies. Furthermore, we have demonstrated spontaneous restoration of platelet GPVI expression in one of these two patients. Thus, GPVI deficiency is an acquired abnormality in these two patients. Although molecular abnormalities in the GPVI gene have been identified in at least two patients with congenital GPVI deficiency [13,14], an immunologic mechanism has been suggested for the pathogenesis of acquired GPVI deficiency. Except for the congenital cases, nine of 11 GPVI-deficient patients, including our new case, have mild or severe thrombocytopenia, which improved with prednisolone treatment [4,6–12]. Indeed, plasma anti-GPVI antibodies have been demonstrated in five cases [4,8,10,12,15]. Nonetheless, no detectable plasma anti-GPVI antibodies were detected in the remaining cases. It has been well established that platelet-associated rather than plasma autoantibodies play a critical role in the pathogenesis of ITP [26,34]. However, the presence of platelet-associated anti-GPVI antibodies is unexpected in patients with GPVI deficiency. We propose that the high affinity of the antibodies in the two patients in this study and/or the high sensitivity of our method using GPVI–FcRγ CHO cells enabled the detection of the anti-GPVI antibodies bound to the residual surface GPVI. Another possible explanation for the successful detection of platelet-associated anti-GPVI antibodies may be that we are detecting internalized anti-GPVI antibodies as discussed below.

Recent reports have demonstrated that there are at least two distinct mechanisms for GPVI downregulation induced by the binding of anti-GPVI antibodies: shedding by activated metalloprotease, and internalization/degradation [18,19]. GPVI is

shed near the transmembrane domain by a metalloprotease after binding of ligands or anti-GPVI antibodies, resulting in the production of an ~ 55-kDa soluble ectodomain fragment and an ~ 10-kDa platelet-associated remnant fragment [31]. In this regard, GPVI shedding has been clearly demonstrated in a GPVI-deficient patient with plasma anti-GPVI antibodies capable of inducing platelet aggregation [12]. In contrast, we failed to detect the membrane-associated remnant GPVI fragment in platelet lysates in our cases (Figs 2D and 5B). GPVI ligation causes not only GPVI–FcRγ shedding, but also calpain-dependent cleavage of FcγRIIA, another ITAM-containing receptor in platelets [12,35]. Again, we failed to detect FcγRIIA cleavage (Figs 2F and 5C). These results suggest that GPVI shedding was not the main cause of GPVI depletion, at least in our cases. GPVI expression in case 1 platelets in November 2006 was estimated to be < 5% by flow cytometry using 204-11 and 5% or less by western blotting using biotinylated convulxin or 204-11, whereas it was estimated to be more than 10% by western blotting using the anti-GPVI cytoplasmic tail antibody. Convulxin and 204-11 binding are tertiary structure-dependent, whereas anti-GPVI cytoplasmic tail antibody binding is not. Thus, this discrepancy may reflect GPVI internalization, as anti-GPVI cytoplasmic tail antibody would detect internalized GPVI complexed with anti-GPVI antibodies. This may explain why we could detect platelet-associated anti-GPVI antibodies despite a marked reduction in the expression of GPVI on the platelet surface, as ether treatment of platelets for antibody elution lyses the plasma membrane. In this context, it has been demonstrated that internalized platelet JAQ1 and GPVI were detectable as long as 48 h after JAQ1 treatment in mice [18]. Moreover, this property of human antibodies is similar to that of the recently reported mouse monoclonal anti-GPVI antibody mF1232, which induces downregulation of GPVI in monkeys without inducing GPVI shedding [19].

Restoration of GPVI expression appeared to be associated with remission of the ITP and the decrease in platelet-associated anti-GPVI autoantibodies relative to GPVI expression. In addition to this case, a meeting abstract has reported partial restoration of GPVI in a GPVI-deficient patient with systemic lupus erythematosus and plasma anti-GPVI antibodies after immunosuppressive therapy [15] These data strongly support an immunologic etiology of GPVI deficiency. However, we could still observe anti-GPVI autoantibodies in eluates obtained in September 2008, despite a marked increase in GPVI expression. Like anti-$\alpha_{IIb}\beta_3$ or anti-GPIb autoantibodies in thrombocytopenia [26,36], anti-GPVI autoantibodies may be heterogeneous in terms of GPVI internalization. In this context, it is noteworthy that *in vivo* administration of some monoclonal anti-GPVI antibodies, such as OM2, OM4, and 9O12.2, does not induce GPVI depletion [37–39]. Alternatively, factors other than antibody binding might be necessary for GPVI deficiency. Further investigation is necessary for a complete understanding of the immunologic mechanisms resulting in GPVI depletion.

Our results also demonstrate that collagen-induced platelet aggregation was dramatically improved in case 1 in February 2008, with only a slight increase of surface GPVI expression (9% of normal). In a mouse model, expression of ~ 20% of control GPVI is sufficient for normal thrombus formation on a collagen-coated surface [40]. These results suggest that even a marked decrease in GPVI expression in platelets might be overlooked in many ITP patients. This possibility is under investigation in our laboratory.

In summary, we have shown for the first time the presence of platelet-associated anti-GPVI antibodies in GPVI-deficient patients. We also demonstrate the restoration of GPVI expression associated with the remission of ITP and a decrease in platelet-associated anti-GPVI autoantibodies. Our present findings thus provide strong evidence for an autoimmune mechanism in the pathophysiology of acquired GPVI deficiency. Moreover, our findings may not only serve to clarify the mechanism of GPVI depletion, but may also lead to the development of new anti-GPVI reagents for the prevention of atherothrombosis.

Acknowledgements

We thank J. Kambayashi, Y. Matsumoto and H. Takizawa (Otsuka Maryland Medicinal Laboratories) for generously providing CHO cells stably expressing GPVI and FcRγ-chain (GPVI–FcRγ CHO cells) and for the soluble form of recombinant human GPVI (amino acids 24–219). This study was supported in part by a Grant-in-Aid for Scientific Research from the Ministry of Education, Culture, Sports, Science and Technology in Japan, by the Ministry of Health, Labor and Welfare in Japan, and by the 'Academic Frontier' Project in Japan.

Disclosure of Conflict of Interests

The authors state that they have no conflict of interest.

References

1 Nieswandt B, Watson SP. Platelet–collagen interaction: is GPVI the central receptor? *Blood* 2003; **102**: 449–61.
2 Moroi M, Jung SM. Platelet glycoprotein VI: its structure and function. *Thromb Res* 2004; **114**: 221–33.
3 Watson SP, Auger JM, McCarty OJ, Pearce AC. GPVI and integrin αIIbβ3 signaling in platelets. *J Thromb Haemost* 2005; **3**: 1752–62.
4 Sugiyama T, Okuma M, Ushikubi F, Sensaki S, Kanaji K, Uchino H. A novel platelet aggregating factor found in a patient with defective collagen-induced platelet aggregation and autoimmune thrombocytopenia. *Blood* 1987; **69**: 1712–20.
5 Moroi M, Jung SM, Okuma M, Shinmyozu K. A patient with platelets deficient in glycoprotein VI that lack both collagen-induced aggregation and adhesion. *J Clin Invest* 1989; **84**: 1440–5.
6 Ryo R, Yoshida A, Sugano W, Yasunaga M, Nakayama K, Saigo K, Adachi M, Yamaguchi N, Okuma M. Deficiency of P62, a putative collagen receptor, in platelets from a patient with defective collagen-induced platelet aggregation. *Am J Hematol* 1992; **39**: 25–31.
7 Arai M, Yamamoto N, Moroi M, Akamatsu N, Fukutake K, Tanoue K. Platelets with 10% of the normal amount of glycoprotein VI have an impaired response to collagen that results in a mild bleeding tendency. *Br J Haematol* 1995; **89**: 124–30.

8 Takahashi H, Moroi M. Antibody against platelet membrane glycoprotein VI in a patient with systemic lupus erythematosus. *Am J Hematol* 2001; **67**: 262–7.

9 Nurden P, Jandrot-Perrus M, Combrié R, Winckler J, Arocas V, Lecut C, Pasquet JM, Kunicki TJ, Nurden AT. Severe deficiency of glycoprotein VI in a patient with gray platelet syndrome. *Blood* 2004; **104**: 107–14.

10 Boylan B, Chen H, Rathore V, Paddock C, Salacz M, Friedman KD, Curtis BR, Stapleton M, Newman DK, Kahn ML, Newman PJ. Anti-GPVI-associated ITP: an acquired platelet disorder caused by autoantibody-mediated clearance of the GPVI/FcRγ-chain complex from the human platelet surface. *Blood* 2004; **104**: 1350–5.

11 Kojima H, Moroi M, Jung SM, Goto S, Tamura N, Kozuma Y, Suzukawa K, Nagasawa T. Characterization of a patient with glycoprotein (GP) VI deficiency possessing neither anti-GPVI autoantibody nor genetic aberration. *J Thromb Haemost* 2006; **4**: 2433–42.

12 Gardiner EE, Al-Tamimi M, Mu FT, Karunakaran D, Thom JY, Moroi M, Andrews RK, Berndt MC, Baker RI. Compromised ITAM-based platelet receptor function in a patient with immune thrombocytopenic purpura. *J Thromb Haemost* 2008; **6**: 1175–82.

13 Freson K, Hermans C, Thys C, van Geet C. GPVI mutation and absent platelet collagen activation in a patient with a bleeding disorder. *Blood* 2007;**110**:627a (abstract).

14 Jandrot-Perrus M, Dumont B, Lasne D, Rothschild C, Grandchamp B, Ajzenberg N. Absent collagen-induced platelet activation in a patient double heterozygous for two GPVI mutations. *Blood* 2008;**112**:39 (abstract).

15 Nurden P, Tandon N, Takizawa H, Gong X, Conception A, Morel D, Merville P, Loya S, Jandrot-Perrus M, Nurden AT. Regulation of an acquired inhibitor to the GPVI platelet collagen receptor in a patient with an autoimmune syndrome and kidney disease. *Blood* 2008;**112**:1168 (abstract).

16 Arthur JF, Dunkley S, Andrews RK. Platelet glycoprotein VI-related clinical defects. *Br J Haematol* 2007; **139**: 363–72.

17 Nieswandt B, Schulte V, Bergmeier W, Mokhtari-Nejad R, Rackebrandt K, Cazenave JP, Ohlmann P, Gachet C, Zirngibl H. Long-term antithrombotic protection by in vivo depletion of platelet glycoprotein VI in mice. *J Exp Med* 2001; **193**: 459–69.

18 Rabie T, Varga-Szabo D, Bender M, Pozgaj R, Lanza F, Saito T, Watson SP, Nieswandt B. Diverging signaling events control the pathway of GPVI down-regulation in vivo. *Blood* 2007; **110**: 529–35.

19 Takayama H, Hosaka Y, Nakayama K, Shirakawa K, Naitoh K, Matsusue T, Shinozaki M, Honda M, Yatagai Y, Kawahara T, Hirose J, Yokoyama T, Kurihara M, Furusako S. A novel antiplatelet antibody therapy that induces cAMP-dependent endocytosis of the GPVI/Fc receptor gamma-chain complex. *J Clin Invest* 2008; **118**: 1785–95.

20 Boylan B, Berndt MC, Kahn ML, Newman PJ. Activation-independent, antibody-mediated removal of GPVI from circulating human platelets: development of a novel NOD/SCID mouse model to evaluate the in vivo effectiveness of anti-human platelet agents. *Blood* 2006; **108**: 908–14.

21 Moroi M, Mizuguchi J, Kawashima S, Nagamatsu M, Miura Y, Nakagaki T, Ito K, Jung SM. A new monoclonal antibody, mAb 204-11, that influences the binding of platelet GPVI to fibrous collagen. *Thromb Haemost* 2003; **89**: 996–1003.

22 Arthur JF, Shen Y, Kahn ML, Berndt MC, Andrews RK, Gardiner EE. Ligand binding rapidly induces disulfide-dependent dimerization of glycoprotein VI on the platelet plasma membrane. *J Biol Chem* 2007; **282**: 30434–41.

23 Jung SM, Ohnuma M, Watanabe N, Sonoda M, Handa M, Moroi M. Analyzing the mechanism of Rap1 activation in platelets: Rap1 activation is related to the release reaction mediated through the collagen receptor GPVI. *Thromb Res* 2006; **118**: 509–21.

24 Honda S, Tomiyama Y, Shiraga M, Tadokoro S, Takamatsu J, Saito H, Kurata Y, Matsuzawa Y. A two-amino acid insertion in the Cys146–Cys167 loop of the αIIb subunit is associated with a variant of Glanzmann thrombasthenia. Critical role of Asp163 in ligand binding. *J Clin Invest* 1998; **102**: 1183–92.

25 Matsumoto Y, Takizawa H, Gong X, Le S, Lockyer S, Okuyama K, Tanaka M, Yoshitake M, Tandon NN, Kambayashi J. Highly potent anti-human GPVI monoclonal antibodies derived from GPVI knockout mouse immunization. *Thromb Res* 2007; **119**: 319–29.

26 Kosugi S, Tomiyama Y, Honda S, Kato H, Kiyoi T, Kashiwagi H, Kurata Y, Matsuzawa Y. Platelet-associated anti-GPIIb–IIIa autoantibodies in chronic immune thrombocytopenic purpura recognizing epitopes close to the ligand-binding site of glycoprotein (GP) IIb. *Blood* 2001; **98**: 1819–27.

27 Kashiwagi H, Tomiyama Y, Kosugi S, Shiraga M, Lipsky RH, Kanayama Y, Kurata Y, Matsuzawa Y. Identification of molecular defects in a subject with type I CD36 deficiency. *Blood* 1994; **83**: 3545–52.

28 Kurata Y, Hayashi S, Kosugi S, Kashiwagi H, Tomiyama Y, Kanayama Y, Matsuzawa Y. Elevated platelet-associated IgG in SLE patients due to anti-platelet autoantibody: differentiation between autoantibodies and immune complexes by ether elution. *Br J Haematol* 1993; **85**: 723–8.

29 Kiyoi T, Tomiyama Y, Honda S, Tadokoro S, Arai M, Kashiwagi H, Kosugi S, Kato H, Kurata Y, Matsuzawa Y. A naturally occurring Tyr143His αIIb mutation abolishes αIIbβ3 function for soluble ligands but retains its ability for mediating cell adhesion and clot retraction: comparison with other mutations causing ligand-binding defects. *Blood* 2003; **101**: 3485–91.

30 Tomiyama Y, Kekomäki R, McFarland J, Kunicki TJ. Antivinculin antibodies in sera of patients with immune thrombocytopenia and in sera of normal subjects. *Blood* 1992; **79**: 161–8.

31 Gardiner EE, Karunakaran D, Shen Y, Arthur JF, Andrews RK, Berndt MC. Controlled shedding of platelet glycoprotein (GP)VI and GPIb–IX–V by ADAM family metalloproteinases. *J Thromb Haemost* 2007; **5**: 1530–7.

32 Kambayashi J, Shinoki N, Nakamura T, Ariyoshi H, Kawasaki T, Sakon M, Monden M. Prevalence of impaired responsiveness to epinephrine in platelets among Japanese. *Thromb Res* 1996; **81**: 85–90.

33 Croft SA, Samani NJ, Teare MD, Hampton KK, Steeds RP, Channer KS, Daly ME. Novel platelet membrane glycoprotein VI dimorphism is a risk factor for myocardial infarction. *Circulation* 2001; **104**: 1459–63.

34 Fujisawa K, Tani P, Pilo L, McMillan R. The effect of therapy on platelet-associated autoantibody in chronic immune thrombocytopenic purpura. *Blood* 1993; **81**: 2872–7.

35 Gardiner EE, Karunakaran D, Arthur JF, Mu FT, Powell MS, Baker RI, Hogarth PM, Kahn ML, Andrews RK, Berndt MC. Dual ITAM-mediated proteolytic pathways for irreversible inactivation of platelet receptors: de-ITAM-izing FcγRIIa. *Blood* 2008; **111**: 165–74.

36 McMillan R. Antiplatelet antibodies in chronic adult immune thrombocytopenic purpura: assays and epitopes. *J Pediatr Hematol Oncol* 2003; **25**(Suppl. 1): S57–61.

37 Matsumoto Y, Takizawa H, Nakama K, Gong X, Yamada Y, Tandon NN, Kambayashi J. Ex vivo evaluation of anti-GPVI antibody in cynomolgus monkeys: dissociation between anti-platelet aggregatory effect and bleeding time. *Thromb Haemost* 2006; **96**: 167–75.

38 Li H, Lockyer S, Concepcion A, Gong X, Takizawa H, Guertin M, Matsumoto Y, Kambayashi J, Tandon NN, Liu Y. The Fab fragment of a novel anti-GPVI monoclonal antibody, OM4, reduces in vivo thrombosis without bleeding risk in rats. *Arterioscler Thromb Vasc Biol* 2007; **27**: 1199–205.

39 Ohlmann P, Hechler B, Ravanat C, Loyau S, Herrenschmidt N, Wanert F, Jandrot-Perrus M, Gachet C. Ex vivo inhibition of thrombus formation by an anti-glycoprotein VI Fab fragment in non-human primates without modification of glycoprotein VI expression. *J Thromb Haemost* 2008; **6**: 1003–11.

40 Best D, Senis YA, Jarvis GE, Eagleton HJ, Roberts DJ, Saito T, Jung SM, Moroi M, Harrison P, Green FR, Watson SP. GPVI levels in platelets: relationship to platelet function at high shear. *Blood* 2003; **102**: 2811–18.

ARTICLE IN PRESS

Available online at www.sciencedirect.com

ScienceDirect

PATHOLOGY
RESEARCH AND PRACTICE

ELSEVIER

Pathology – Research and Practice ▮ (▮▮▮▮) ▮▮▮–▮▮▮

www.elsevier.de/prp

TEACHING CASES

Peripheral T-cell lymphoma of Lennert type complicated by monoclonal proliferation of large B-cells ☆

Takeshi Chihara[a], Naoki Wada[a], Masaharu Kohara[a], Takako Matsui[b], Hiroaki Masaya[b], Tetsuo Maeda[b], Hirohiko Shibayama[b], Yuzuru Kanakura[b], Mamori Tani[c], Eiichi Morii[a], Katsuyuki Aozasa[a,*]

[a]*Department of Pathology (C3), Osaka University Graduate School of Medicine, 2-2 Yamadaoka, Suita, Osaka 565-0871, Japan*
[b]*Department of Hematology and Oncology, Osaka University Graduate School of Medicine, 2-2 Yamadaoka, Suita, Osaka 565-0871, Japan*
[c]*Department of Dermatology, Osaka University Graduate School of Medicine, 2-2 Yamadaoka, Suita, Osaka 565-0871, Japan*

Received 3 February 2009; received in revised form 3 April 2009; accepted 22 April 2009

Abstract

A 69-year-old man presented with lymph node swelling in the right inguinal region. A biopsy was made (LN1) and diagnosed as peripheral T-cell lymphoma. The lesion remitted completely over a period of about 51 months after combination chemotherapy, but erythematous papules, systemic lymphadenopathy, and fever of 38° appeared. Skin (S1) and lymph nodes (LN2) were biopsied. Erythematous papules once disappeared spontaneously, but appeared again and were biopsied (S2). LN1 displayed the typical histologic and immunohistochemical features of Lennert lymphoma, i.e., diffuse proliferation of small to large lymphoid cells of CD3+, CD4+, CD8− immunophenotype accompanied by numerous clusters of epithelioid histiocytes. In LN2, the large cells with CD3+, CD4+, CD8− decreased in number, while numerous CD20+ large cells were discernible. Clonality analysis revealed the persistent presence of an identical T-cell clone in LN1 and LN2. Clonal bands of immunoglobulin heavy (IgH) chain gene were detected in LN2 but not in LN1. S1 and S2 showed diffuse proliferation of small to large lymphoid cells of CD20−, CD3+, CD4+, CD8− in the upper dermis, with obvious epidermotropism. Clonality analysis revealed the presence of a T-cell clone identical to LN1 and LN2 with no B-cell clone, indicating the recurrence of PTCL. In situ hybridization (ISH) for Epstein-Barr virus (EBV) genome revealed that positive signals in the nucleus of large B-lymphoid cells appeared only in LN2.

Taken together, EBV-positive large B-cell lymphoma appeared transiently in the course of "Lennert lymphoma".

Keywords: Peripheral T-cell lymphoma of Lennert type; Clonality analysis; Secondary B-cell lymphoma; Epstein-Barr virus

☆ Supported in part by a grant (200114012) from the Ministry of Education, Culture, Sports, Science and Technology, Japan.
*Corresponding author.
E-mail address: aozasa@molpath.med.osaka-u.ac.jp (K. Aozasa).

0344-0338/$ - see front matter © 2009 Elsevier GmbH. All rights reserved.
doi:10.1016/j.prp.2009.04.009

Please cite this article as: T. Chihara, et al., Peripheral T-cell lymphoma of Lennert type complicated by monoclonal proliferation of large B-cells, Pathol. Res. Practice (2009), doi:10.1016/j.prp.2009.04.009

Introduction

Evolution of B-cell lymphoma during the course of peripheral T-cell lymphoma (PTCL) is regarded as a relatively rare event. Recently, however, reports of such cases have accumulated [4,5,10]. Angioimmunoblastic T-cell lymphoma (AILT) is the PTCL representative for the development of secondary B-cell lymphoma. An immunodeficient condition induced in AILT might be responsible for the evolution of B-cell lymphoma because evolving B-cell lymphomas usually have a large cell morphology and contain Epstein-Barr virus (EBV) genome [2,9], common findings in B-cell lymphomas developing in immunocompromised hosts.

Here we report a well-characterized case of PTCL of Lennert type, in which diffuse large B-cell lymphoma (DLBCL) evolved transiently. This report is the first to describe the evolution of B-cell lymphoma during the course of Lennert lymphoma, justified not only by morphology but also on a molecular basis. The clinical relevance of this case is discussed.

Case report

A 69-year-old man with a history of diabetes mellitus had noticed lymph node swelling in the right inguinal region. Two months later, he was admitted with bilateral cervical and inguinal lymphadenopathy and fever of 38°. Neither hepatosplenomegaly, night sweats, weight loss nor skin rash was observed. Laboratory findings including peripheral blood counts and differentials and serum lactate dehydrogenase (LDH) were normal. Gammopathy in the serum was absent. Soluble interleukin 2 receptor (sIL-2R) was 907 U/ml. The left inguinal lymph node was biopsied and diagnosed as peripheral T-cell lymphoma (LN1). Combination chemotherapy (cyclophosphamide, doxorubicin, vincristine, and prednisone) was started under the diagnosis of PTCL, stage III. After completion of 6 courses, the lymphadenopathy regressed completely over a period of about 51 months. Then, pain-causing erythematous papules appeared in the bilateral palms and soles, accompanied by systemic lymphadenopathy and fever of 38°. Neither hepatosplenomegaly, night sweats nor loss of weight was observed. There was slight anemia. Serum LDH and sIL-2R were elevated: 843/U and 2862 U/ml, respectively. The skin of the left palm and lymph nodes in the neck and inguinal region were biopsied (S1 and LN2). Erythematous papules disappeared spontaneously. LN2 was diagnosed as composite PTCL and DLBCL. Combination chemotherapy (Rituximab, pirarubicin, cyclophosphamide, vincristine, and prednisone) was started, but pneumocystis jiroveci and cytomegalovirus pneumonia evolved. After two courses of chemotherapy, the pneumonia was improved by administration of ganciclovir, co-trimoxazole, and prednisone, but continuation of the chemotherapy was difficult. The erythematous papules reappeared in the whole body, with severe edema in the face and extremities: the skin of the right thigh was biopsied (S2). Finally, a leukemic picture of $CD2^+$, 3^+, 4^+, $CD19^-$, and $CD20^-$ cells appeared in the peripheral blood (64% of leukocytes) together with progressive systemic lymphadenopathy and splenomegaly. The patient died 4 months after the diagnosis of composite PTCL and DLBCL.

Materials and methods

Biopsy samples (LN1, LN2, S1, S2) were fixed in 10% formalin and routinely processed for paraffin-embedding. Histologic sections cut at 4 μm were stained with hematoxylin and eosin and immunoperoxidase procedure (avidin–biotin complex method). Primary antibodies used for immunophenotyping were CD20, CD79a, CD3, CD8, bcl6 (Dakocytomation, Glostrup, Denmark, dilution of 1:400, 1:100, 1:50, 1:100, 1:50, respectively), CD10 (Nichirei Biosciences, Tokyo, Japan, used as a prediluted antibody) and CD4 (Novocastra Laboratories, Newcastle, UK, 1:40).

Clonality analysis

DNA was extracted from the paraffin-embedded samples from LN1, LN2, S1 and S2 as described previously [7]. To evaluate clonality for B-cells and T-cells, PCR was performed, i.e., a BIOMED-2 PCR protocol was applied as described previously [7]. The amplified products were electrophorezed in 6% polyacrylamide gel. A case of lymphoid follicular hyperplasia of tonsil was included as a polyclonal control.

In situ hybridization (ISH)

RNA in situ hybridization using the EBER-1 (Epstein-Barr encoded RNAs) probe was performed to examine the presence of EBV genome on the formalin-fixed, paraffin-embedded sections according to the previously described method with some modifications [8].

Double staining for immunophenotype and ISH for EBV genome

To determine the B- or T-cell nature of EBV-infected cells, we performed a double-labeling procedure using immunohistochemistry and EBER-ISH. Immunohistochemical detection of CD20 and CD3 antigens was

Please cite this article as: T. Chihara, et al., Peripheral T-cell lymphoma of Lennert type complicated by monoclonal proliferation of large B-cells, Pathol. Res. Practice (2009), doi:10.1016/j.prp.2009.04.009